Polymerization and Characterization of 4,4′-Bis(alkylsulfanyl)-2,2′-bithiophenes

Dario Iarossi, Adele Mucci, Luisa Schenetti,* and Renato Seeber

Dipartimento di Chimica, Università di Modena, via Campi 183, I-41100 Modena, Italy

Francesca Goldoni

Laboratory of Macromolecules and Organic Chemistry, Department of Chemistry, Technische Universiteit Eindhoven, Postbus 513, Eindhoven, The Netherlands

Marco Affronte and Filippo Nava

I.N.F.M. and Dipartimento di Fisica, Università di Modena, via Campi 213a, I-41100 Modena, Italy

Received August 25, 1998; Revised Manuscript Received December 8, 1998

ABSTRACT: Regioregular polymers poly[4,4′-bis(butylsulfanyl)-2,2′-bithiophene] (**P1**) and poly[4,4′-bis(octylsulfanyl)-2,2′-bithiophene] (**P2**) were prepared from 4,4′-bis(butylsulfanyl)- and 4,4′-bis(octylsulfanyl)-2,2′-bithiophene, by oxidative polymerization with $FeCl_3$, and characterized by ^1H and ^{13}C NMR, FT-IR, and UV−vis spectroscopies, atomic force microscopy (AFM), electrical conductivity, and cyclic voltammetry measurements. They exhibit weight-average molecular weights of 8 and 70 kDa, respectively, and are both readily soluble in $CHCl_3$, CH_2Cl_2, CS_2, toluene, and THF. **P1** has a lamellar structure, and **P2** is a flexible and compact film that can be easily processed and manipulated. In the neutral state, they show UV−vis absorption maxima at about 470 nm in $CHCl_3$ solution and exhibit marked solvatochromism and thermochromism. Furthermore, they can be cast from orange-red solution to form a violet film. The p-doping potentials have been determined, and the possibility of electrogenerating corresponding polymers has been checked. First comparative characterizations of the electrogenerated polymers have been carried out.

Introduction

Poly(3-alkylthiophene)s can be chemically or electrochemically synthesized[1] from the corresponding 3-alkylthiophenes, but the related polymers can suffer from different regiochemistry, due to different possible coupling between the 2- and 5-positions of the monomer. Regioregular head-to-tail (HT) polythiophenes can be generated through the synthetic methods described by McCullough[1] and Rieke.[2] Otherwise, polymers with a regioregular head-to-head/tail-to-tail (HH−TT) structure can be synthesized from symmetrical 3,3′- or 4,4′-disubstituted-2,2′-bithiophenes.[3−5]

Polythiophenes carrying electron-donating alkylsulfanyl groups are less documented than poly(3-substituted thiophene)s carrying substituents such as alkyl, alkoxy, and alkyl heteroatom-functionalized side chains.[1] The synthesis of a series of regioregular poly[3-(alkylsulfanyl)thiophene]s with low molecular weights has appeared[2,6,7] whereas recent papers have reported the chemical[8a,9] and the electrochemical[8b] polymerization of 3,3′-bis(alkylsulfanyl)-2,2′-bithiophenes and evidenced the facile n- and p-dopability of the synthesized polymers.

We report here on the polymerization and characterization of 4,4′-bis(butylsulfanyl)- (**2a**) and 4,4′-bis(octylsulfanyl)-2,2′-bithiophene (**2b**) by oxidative coupling with $FeCl_3$. The oxidative method afforded polymers poly[4,4′-bis(butylsulfanyl)-2,2′-bithiophene] (**P1**) and poly[4,4′-bis(octylsulfanyl)-2,2′-bithiophene] (**P2**) with molecular weight of 8 and 70 kDa, respectively. The polymers are soluble in common organic solvents such as $CHCl_3$, CCl_4, toluene, benzene, THF, and CS_2. Electrosynthesis of poly[4,4′-bis(butylsulfanyl)-2,2′-bithiophene] (**P1E**) and poly[4,4′-bis(octylsulfanyl)-2,2′-bithiophene] (**P2E**) and electrochemical characterization of both electrogenerated and chemically prepared polymers are also reported. In particular, electrogenerated polymers have been preliminarily analyzed by UV−vis spectroscopy.

Experimental Section

4,4′-Bis(butylsulfanyl)-2,2′-bithiophene (2a). The dimer was obtained from the corresponding dibromo derivative, as previously reported.[10]

4,4′-Bis(octylsulfanyl)-2,2′-bithiophene (2b). The synthesis was carried out according to the literature method.[11] A solution of octan-1-thiol (6.3 g, 43.2 mmol) in DMSO (21 mL) was added with stirring to NaH (1.0 g, 43.2 mmol) under a flow of dry nitrogen. When the evolution of the H_2 gas ceased, CuO (0.2 g), KI (0.2 g), and a solution of 4,4′-dibromo-2,2′-bithiophene (3.5 g, 10.8 mmol) in DMSO (21 mL) were added. The resulting mixture, stirred at 10 °C for 15 h, was cooled, poured onto ice water, and added with $CHCl_3$ (100 mL). The aqueous layer was extracted with $CHCl_3$ (100 mL), and the combined organic layers were washed with brine and water and dried ($MgSO_4$). The solvent was removed, and the crude product was chromathographed on silica gel (previously neutralized by flowing with 2% triethylamine through), using light petroleum (bp 40−70 °C) as the eluant. The yellow solid was recrystallized from pentane: 1.38 g, 36% yield; mp 62−64 °C. ^1H NMR (400.13 MHz, $CDCl_3$; Me_4Si): δ 7.06 (d, 1H, J_{35} 1.5 Hz, 3-H), 6.99 (d, 1H, J_{35} 1.5 Hz, 5-H), 2.85 (m, 2H, $CH_2(\alpha)$), 1.64 (m, 2H, $CH_2(\beta)$), 1.42 (m, 2H, $CH_2(\gamma)$), 1.27 (m, 6H, 3 × CH_2), 0.88 (t, 3H, CH_3). ^{13}C NMR ($CDCl_3$, 100.61 MHz): C-2 137.2, C-3 126.0, C-4 133.2, C-5 121.9, $CH_2(\alpha)$ 35.2, $CH_2(\beta)$ 29.3, $CH_2(\gamma)$ 28.7, $CH_2(\delta)$ 29.1, $CH_2(\epsilon)$ 29.0, $CH_2(\phi)$ 31.7, $CH_2(\omega)$ 35.2, and CH_3 14.0. Anal. Calcd for $C_{24}H_{38}S_4$: C, 63.38; H, 8.42; S, 28.2. Found: C, 63.5; H, 8.2; S, 28.3.

Poly[4,4′-bis(butylsulfanyl)-2,2′-bithiophene] (P1). To a stirred solution of **2a** (1.14 g, 3.3 mmol) in $CHCl_3$ (50 mL) a

10.1021/ma9813340 CCC: $18.00
Published on Web 02/11/1999

solution of $FeCl_3$ (2.2 g, 13.5 mmol) in CH_3NO_2 (50 mL) was dropwise added (2 h), under a flow of dry nitrogen. The greenish mixture was stirred for 20 h at room temperature and evaporated. The residue was stirred (1 h) with a solution of HCl acidified methanol (50 mL). The dark product was centrifuged, washed with methanol, and Soxhlet-extracted with methanol (24 h), *n*-pentane (30 h), and $CHCl_3$ (40 h). Methanol and pentane were removed under vacuum to afford oligomeric fractions of the polymer. The purplish $CHCl_3$ solution (250 mL) was concentrated nearly to dryness, and 20 mL of methanol was added to give on the glassware the polymer (0.4 g, 35% yield) as a dark greenish-golden friable film, easy to detach. The product collected, washed with methanol, and dried in vacuo is soluble in common organic solvents such as $CHCl_3$, CH_2Cl_2, CCl_4, CS_2, benzene, toluene, and THF at room temperature.

Poly[4,4′-bis(octylsulfanyl)-2,2′-bithiophene] (P2). The polymer was prepared from **2b** (0.7 g, 1.54 mmol) according to the procedure adopted for **P1**. After usual workup procedure, the $CHCl_3$ solution (180 mL) was concentrated nearly to dryness, and methanol (20 mL) was added to give **P2** (0.68 g, 97% yield) as free-standing greenish-golden film. This polymeric film is a flexible material that can only be cut by scissors.

Measurements. UV−vis spectra were recorded on a Varian-Cary 5E spectrophotometer, except for the case of thermochromic measurements, performed with a Perkin-Elmer Lambda 900 spectrophotometer. ^1H and ^{13}C NMR measurements were performed on a $CDCl_3$ polymer solution with a Bruker AMX-400 WB spectrometer operating at 400.13 and 100.61 MHz, respectively, or with a Bruker Avance DPX-200 instrument operating at 200.13 and 50.31 MHz, respectively. The ^1H and ^{13}C chemical shifts (δ, ppm) are quoted with respect to the $CHCl_3$ signal at 7.26 ppm (for ^1H) and the $^{13}CDCl_3$ signal at 77.0 ppm (for ^{13}C). FT-IR spectra were recorded using a Perkin-Elmer i-series FT-IR microscope.

Gel permeation chromatography (GPC) was carried out using an Hewlett-Packard system equipped with a Plgel column and a diode-array UV detector, with THF as the eluant, at room temperature. The average molecular weights were calculated using a calibration curve of monodisperse polystyrene standards. Thermal gravimetric analysis (TGA) was performed with a Perkin-Elmer TGA7 instrument, at a scan rate of 10 °C min^{-1}. Atomic force microscopic (AFM) 256 × 256 pixel images were recorded at ambient conditions with a Park Autoprobe CP scanning probe microscope equipped with a cantilever of 0.05 N/m spring constant operating in constant-force contact mode.

Electropolymerizations and electrochemical characterization of both electrogenerated and chemically prepared electrode film coatings were performed using the computerized AUTOLAB PGSTAT20 electrochemical instrument (Ecochemie). All electrochemical tests were carried out at room temperature under nitrogen atmosphere, using a single-compartment, three-electrode cell. The platinum electrode (Goodfellow, 99.99+% pure) was inserted inside a Teflon tube. The electrode was polished with 0.3 and 0.05 μm alumina powder and then rinsed with distilled water and sonicated in an ultrasonic bath for 5 min before use. The working electrode potentials were measured with respect to an aqueous saturated calomel electrode (SCE), unless the use of an aqueous Ag|AgCl(s), KCl(s) [$E_{SCE} = E_{Ag|AgCl,KCl} + 0.040$ V] is specified. A Pt foil was used as counter electrode. Tetrabutylammonium hexafluorophosphate ($TBAPF_6$, 0.1 M, Fluka, puriss.) supporting electrolyte in acetonitrile or acetonitrile/dichloromethane (1/1) solvents (Aldrich, 99.9+ % pure, packaged under nitrogen) was the medium for electrochemical measurements.

The electrical resistance, from which we can obtain resistivity and conductivity, was measured by using a high-voltage electrometer (EIHLEY 237) and a four-point probe of Kulicke & Soffa series 333. The thickness of the **P1** thin film was measured by an Alpha Step-Tencor 200, whereas that of the **P2** thick film by an electronic thickness monitor (TL-202-p).

Results

Chemical Polymerization. The polymers were prepared by oxidative polymerization of **2a** and of **2b** by adapting the experimental procedure described in the literature.[1] Anhydrous $FeCl_3$, in a monomer molar ratio 4/1, was used in dry $CHCl_3/CH_3NO_2$ (1/1), instead of pure chloroform. The choice of the reaction solvents was suggested by the observation that longer oligomers are generated in the oxidative reaction of alkylsulfanyl thiophenes and oligothiophenes with $FeCl_3$, passing from chloroform to chloroform/nitromethane mixtures.[12,13]

Molecular Weights Determination. The molecular weights of **P1** and **P2** were estimated by GPC. **P1** weight-average molecular weight, M_w, and number-average molecular weight, M_n, were 8000 and 4600, respectively, with a polydispersivity index, M_w/M_n, of 1.7. **P2** weight-average molecular weight, M_w, and number-average molecular weight, M_n, were 70 000 and 20 000, respectively, with a polydispersivity index, M_w/M_n, of 3.5. The M_w of polymers **P1** and **P2** correspond to 23 and to more than 150 dimeric units per chain, respectively.

NMR Characterization. ^1H and ^{13}C NMR spectra of **P1** and **P2** in $CDCl_3$ are reported in Figures 1 and 2. The ^1H NMR spectra display, in the aromatic region, a very sharp peak at 7.2 ppm, attributable to H-3 of the thiophene ring. The aliphatic region of **P1** shows four groups of signal at 2.89, 1.63, 1.43, and 0.92 ppm, due to the protons of the alkylsulfanyl chain and assigned to $CH_2(\alpha)$, $CH_2(\beta)$, $CH_2(\gamma)$, and CH_3, respectively. In the aliphatic region of the **P2** spectrum five groups of signals are present, at 2.87, 1.62, 1.39, 1.26, and 0.86 ppm, due to the protons of the octylsulfanyl chain. These signals are assigned to $CH_2(\alpha)$, $CH_2(\beta)$, $CH_2(\gamma)$, to the remaining four CH_2, and to CH_3, respectively. The ^{13}C NMR spectra of **P1** and **P2** display four signals in the aromatic region and four or eight signals in the aliphatic region. Inverse-detected one-bond heteronuclear multiple-quantum correlation experiments (HMQC)[14] allowed us to assign the signal at 127.5 ppm to C-3 carbon, whereas heteronuclear multiple-bond correlation experiments (HMBC)[15] enabled the assignment of the remaining carbons to be performed. The assignment of the aliphatic carbons of **P1** and **P2** was similarly obtained through one-bond and long-range correlations with the aliphatic protons. The NMR results are reported in Table 1. Both proton spectra display in the aromatic region some low signals, whose relative intensities change with the purification procedure, that are attributable to oligomeric chains.

The values of the chemical shifts found for aromatic protons and carbons are diagnostic for the TT-HH triad. In fact, a comparison with NMR data of HT regioregular poly[3-(butylsulfanyl)thiophene][7] shows that the aromatic proton is strongly deshielded (7.37 ppm) with respect to **P1** and **P2**, like H-3′ belonging to the HT dimer (7.27 ppm) is more deshielded with respect to H-3 of the TT dimer (7.06 ppm) in the case of bis(butylsulfanyl)bithiophenes.[10,16] When carbon signals of **P1** and **P2** are compared to those of HT regioregular poly[3-(butylsulfanyl)thiophene],[7] an alternating deshielding/shielding effect is observed, passing from C-2 to C-5. In particular, the protonated aromatic carbon is deshielded (130.3 ppm) whereas the aromatic carbon bearing the alkylsulfanyl group is shielded (129.1 ppm) in the HT polymer with respect to the corresponding signals of **P1**

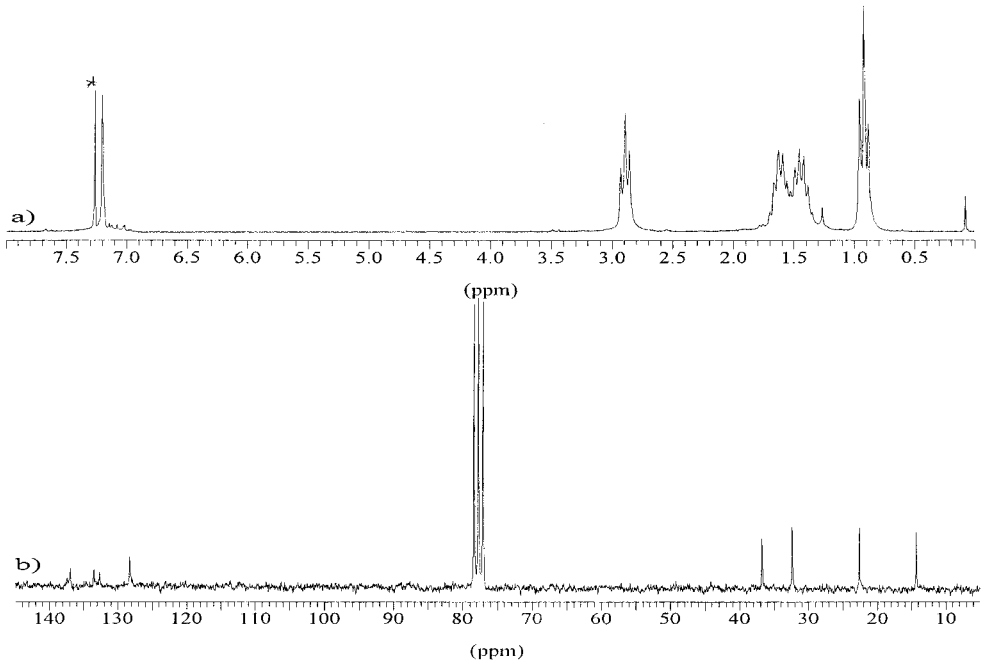

Figure 1. (a) The 200.13 MHz ^{1}H NMR spectrum and (b) 50.31 MHz ^{13}C NMR spectrum of **P1** in $CDCl_3$. The asterisked peak in (a) comes from residual $CHCl_3$.

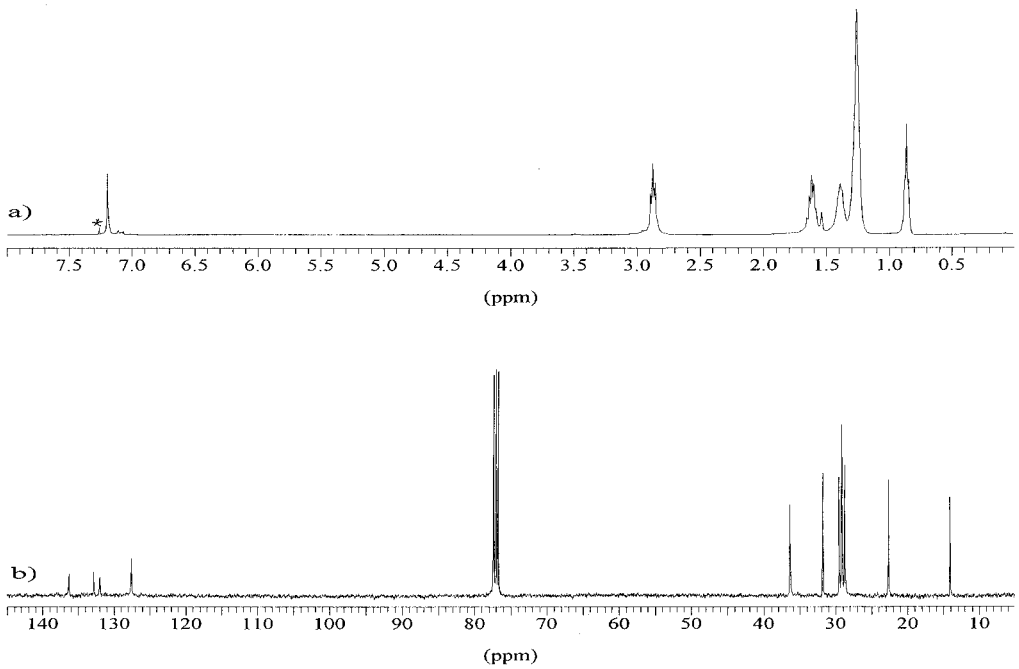

Figure 2. (a) The 400.13 MHz ^{1}H NMR spectrum and (b) 100.61 MHz ^{13}C NMR spectrum of **P2** in $CDCl_3$. The asterisked peak in (a) comes from residual $CHCl_3$.

Table 1. ^{1}H and ^{13}C Chemical Shift (δ_H and δ_C in ppm, TMS) of P1 and P2

	C-2	H-3/C-3	C-4	C-5	$CH_2(\alpha)$	$CH_2(\beta)$	$CH_2(\gamma)$	$CH_2(\delta/\epsilon)$	$CH_2(\phi)$	$CH_2(\omega)$	CH_3
P1		7.20			2.89	1.63	1.43				0.92
	136.3	127.5	132.8	132.0	36.0	31.6	21.9				13.6
P2		7.19			2.87	1.62	1.39	1.26	1.26	1.26	0.86
	136.2	127.5	132.8	131.9	36.4	29.3	28.8	29.2/29.4	31.8	22.6	14.1

and **P2**. These findings confirm the dependence on the regiochemistry of aromatic carbon chemical shifts that has already been observed in the case of polythiophenes bearing β-alkyl chains.[17]

Infrared Spectroscopy. The two native polymers were analyzed with an IR microscope. The IR reflectance spectra show similar features. The alkylsulfanyl chains give rise to stretching vibrations in the region 2960−2850 cm^{-1}, to deformation modes around 1470 and 1370 cm^{-1}, and to C−S stretching absorptions at 932 cm^{-1}. The aromatic C−H_β stretching and out-of-plane deformation are found around 3077 and 815 cm^{-1}, respectively. The thiophene ring stretching contributes to the band at 1470 cm^{-1}.

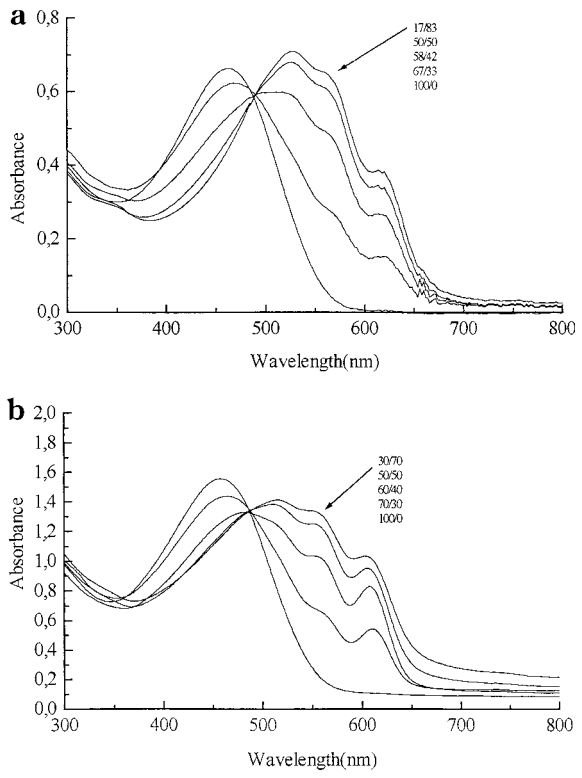

Figure 3. Solution UV−vis spectra of (a) **P1** and (b) **P2** in $CHCl_3/CH_3OH$ mixture. $CHCl_3$ to CH_3OH ratios are indicated.

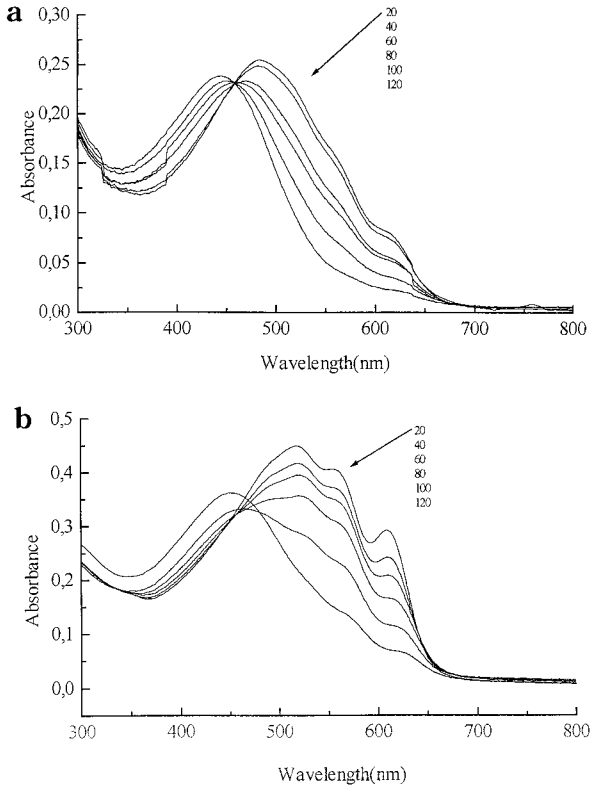

Figure 4. UV−vis spectra in *n*-decanol at different temperatures of (a) **P1** and (b) **P2**.

Solution and Solid-State UV−vis Spectroscopy. The UV−vis spectra of **P1** and **P2** in dilute $CHCl_3$ solutions display absorption maxima at 470 and 466 nm, respectively. Both polymers display strong solvato- and thermochromism. Figure 3a,b shows the UV−vis spectra of **P1** and **P2** in $CHCl_3/CH_3OH$ mixed solvents. The change in color from orange to violet upon addition of the poor solvent, methanol, to a chloroform solution corresponds to the appearance of three new maxima at longer wavelengths, i.e., at about 520, 560, and 610 nm, with an estimated 1.7 eV band-gap value. The solid-state UV−vis absorption spectra of **P1** and **P2** films formed by solvent evaporation on glass from $CHCl_3$ display absorptions similar to those obtained at high $CH_3OH/CHCl_3$ ratios in solution.

The thermochromic properties of **P1** and **P2** were also investigated. In Figure 4a,b the UV−vis spectra of the polymers in *n*-decanol solvent at increasing temperatures are shown. In such a poor solvent, at 20 °C λ_{max} is found at 490 and 520 nm for **P1** and **P2**, respectively, and vibrational fine structure is observed for both polymers. As shown in Figure 4, by increasing the temperature the vibronic fine structure is less and less evident, and the absorption maximum is shifted to higher energies in both polymers. When cooling the solutions the vibronic fine structure is regained, but with some hysteresis.

Similar thermochromic and solvatochromic properties have been reported for regioregular HT poly(3-alkylthiophene)s.[18] A comparative analysis shows that vibrational fine structure is absent in good solvents or at high temperatures but develops when aggregation is induced by lowering the quality of the solvent or the temperature and in the solid state.

Two different, and not necessarily in contrast, models are found in the literature[2,9,18a] to explain this behavior. The former[18a] considers an intrachain mechanism based on the existence of an equilibrium process between an ordered, more extensively conjugated rodlike form, present in poor solvents or at low temperature, and a disordered, less conjugated coillike form, prevailing in good solvent and at high temperature absorbing at shorter wavelength. The latter model[19] considers the formation, in poor solvents or at low temperature, of aggregates in suspension in equilibrium with the polymer in solution. This is an interchain mechanism that can be influenced by intrachain phenomena. In fact, microcrystallization can only occur after the polymer has transformed into a more ordered conformation. A detailed analysis of factors influencing the conformational preferences of HH and HT polythiophenes can be found in a recent paper by Leclerc et al.,[9] in which the thermochromic behavior of a poly[3,3′-bis(butylsulfanyl)-2,2′-bithiophene] in the solid state, very similar to that shown by **P1** in solution, is discussed. Figures 3 and 4 indicate that also **P1** and **P2** exist as mixtures of two forms, one absorbing at a shorter and the other at longer wavelengths, corresponding to a less and a more conjugated form, in equilibrium with each other. The more marked thermochromic effect presented by **P2** with respect to **P1** suggests an enhanced contribution to the stabilization of a planar conformation (at least the antiplanar form)[9] coming from interchain (or intrachain through folding) interactions effective at low temperatures.

The absorption maxima of **P1** and **P2** in $CHCl_3$ solution are about 20 nm red-shifted with respect to regioregular HT poly(3-alkylthiophene)s,[20] but at a wavelength about 40 nm shorter than λ_{max} of regioregular HT poly[3-(alkylsulfanyl)thiophene]s,[2,7] whereas the UV−vis spectra in $CH_3OH/CHCl_3$ solutions and in the solid state are similar to those reported for regioregular HT poly(3-alkylthiophene)s[18g,20,21] and poly[3-(alkylsulfanyl)thiophene]s[2,7] in the solid state.

Marked differences are found when **P1** and **P2** are compared with other HH−TT regioregular poly(β,β′-disubstituted bithiophene)s. Regioregular HH−TT poly(β,β′-dialkylbithiophene)s, in fact, do not present the solvatochromism phenomenon and absorb at shorter wavelengths,[3a,4] whereas minor solvatochromic effects but longer absorption wavelengths are found for polymers obtained from 3,3′-dibutoxy- and 4,4′-dibutoxy-2,2′-bithiophene.[5] These observations can be rationalized on the basis of different conformational behaviors induced by the different substituents, as shown in a recent theoretical paper.[22] Regioregular HH−TT poly(β,β′-dialkyl-2,2′-bithiophene)s retain distorted structures whatever the environment is, poly(β,β′-dialkoxybithiophene)s are almost planar even in chloroform solution, and a mobile situation is found for poly[β,β′-bis(alkylsulfanyl)-2,2′-bithiophene]s.

From the UV−vis study of **P1** and **P2** we can conclude that these polymers adopt more distorted conformations with respect to HH−TT poly(β,β′-dialkoxy-2,2′-bithiophene)s and regioregular HT poly[3-(alkylsulfanyl)-thiophene]s in chloroform solution, whereas, despite the different substituents and regiochemistry, very similar conformations and order are present in $CH_3OH/CHCl_3$ solutions and in the solid state.

Thermogravimetric Analysis. TGA of **P1** and **P2** reveals a limited initial weight loss of 3% and 2%, respectively, between 160 and 210 °C, presumably due to the loss of adsorbed moisture or solvent. The first decomposition process onsets around 250 °C for both polymers. The corresponding weight losses, 36% for **P1** and 52% for **P2**, are ascribable to the elimination of the pendant chains. Decomposition of the polymer backbone begins in both cases at temperatures higher than 450 °C.

Morphological Analysis. P1 and **P2** films were analyzed in their native forms (i.e., as they are obtained from the last purification step—see Experimental Section). From a macroscopic point of view the appearance of the two polymer films is different: **P2** forms flexible and compact glossy films that can be easily cut and manipulated, whereas **P1** forms less glossy brittle scaly films. Both materials were analyzed through AFM, and two topographical images of 4 μm × 4 μm size are shown in Figure 5a,b along with the relevant height profiles. The macroscopically more compact and brilliant **P2** shows, in the AFM image, a smoother surface than **P1**. The higher molecular weight of **P2** can be supposed to favor a better self-alignment of the polymer chains that produces a flatter surface.

Electrical Conductivity. The structures for the conductivity measurements on the polymers prepared by the chemical procedure were fabricated in two different ways. A first structure was built up with the polymer **P1** film, 1.3 μm thick, formed between two copper electrodes deposited on an insulating ($R > 10^{12}$ ohm) ceramic substrate, and the other structure with the polymer **P2**, 75 μm thick, cut in a square shape, 1.5 × 1.5 mm^2, electrically contacted by means of a conductive layer of carbon deposited on the opposite surfaces and supported by a T0-5 header for the microelectronic circuit package. **P1** and **P2** films were p-doped either by exposition to I_2 vapor for 15 h or by immersion in a 0.02 M solution of $FeCl_3$ in nitromethane for 24 h. The conductivities of doped **P1** and **P2** were measured with both a high-voltage electrometer and a square four-probe array centered on a square sample by using the appropriate correction factor.[23] The conductivities of neutral and doped polymers are reported in Table 2.

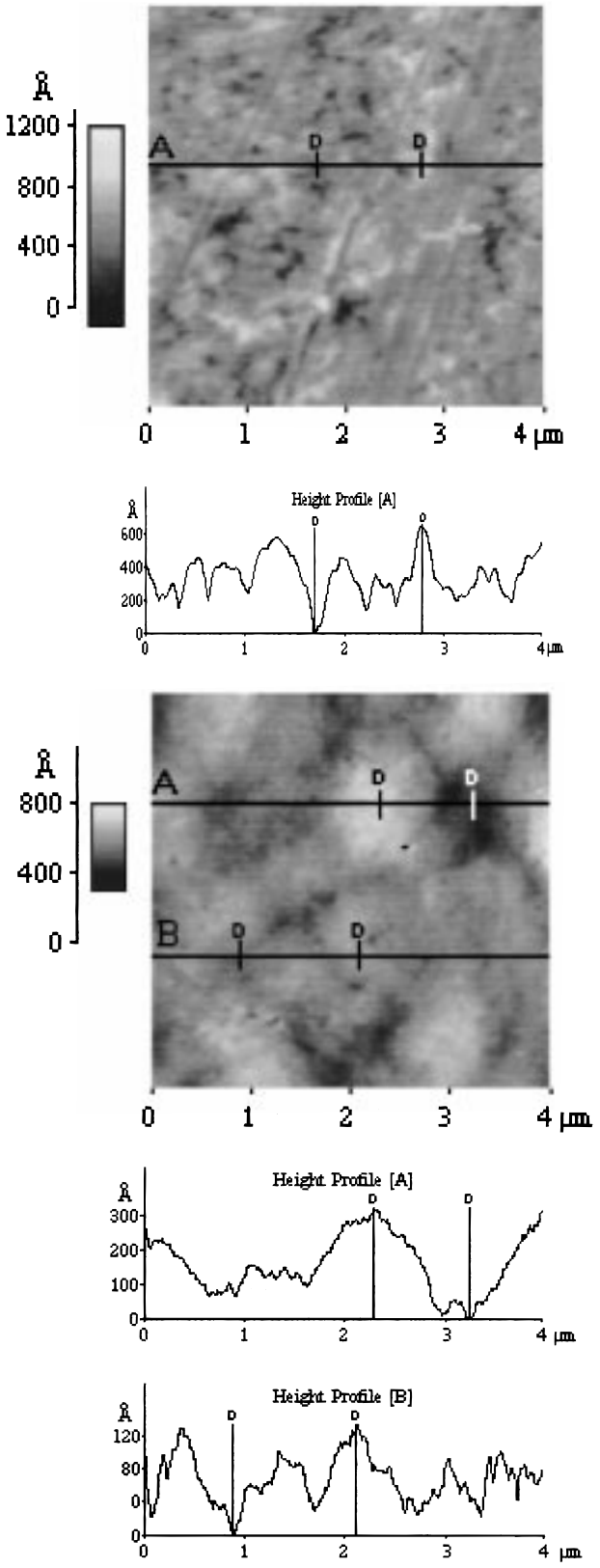

Figure 5. AFM images of (a, upper) **P1** and (b, lower) **P2** (4 μm × 4 μm) are shown along with selected height profiles.

A comparative analysis of the conductivity data collected by using two different measurement devices can be explained by assuming a nonuniform oxidation of the film of the polymers. With the four-probe technique, in fact, the surface conductivity plays the main

Table 2. Electrical Conductivities of the Neutral and Doped Polymers (S/cm)

		I_2-doped		$FeCl_3$-doped	
	pristine	HVE[a]	FP[a]	HVE[a]	FP[a]
P1	2×10^{-8}	3×10^{-3}	0.5	2×10^{-3}	0.7
P2	1.5×10^{-10}	1.5×10^{-5}	0.7	1.6×10^{-5}	1.3

[a] HVE = high-voltage electrometer; FP = four-probe array.

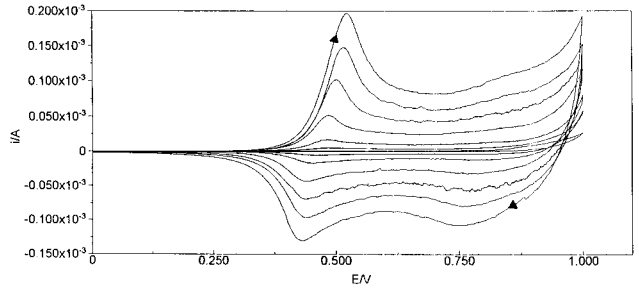

Figure 6. Continuous cycling electropolymerization of MeCN solution of 5×10^{-3} M **2a**. Potential range: 0.0−1.0 V. Curves are recorded every 10 scans; 50 mV s^{-1} potential scan rate; initial anodic scan direction.

role while the bulk conductivity is measured when the electrodes are on the opposite surfaces of a polymer film. Further work is in progress in order to clarify the oxidation process and the observed differences.

The conductivity values obtained through the four-probe method are lower than those reported for regioregular HT−HT poly[3-(alkylsulfanyl)thiophene]s[2] but are similar to those reported for regioregular HH−TT poly(β,β'-dialkyl)- and (β,β'-dialkoxy)bithiophenes.[4,5,24]

Electrosynthesis and Electrochemical Characterization. Electropolymerizations of both monomers were accomplished using $(2.5-5.0) \times 10^{-3}$ M solutions, by repeatedly cycling the electrode potential between the limits +0.00 and +1.00 V for **2a** and +1.10 V for **2b**, at a potential scan rate of 50 mV/s. Electropolymerizations were also carried out on a conducting indium−tin oxide (ITO) glass electrode, on which UV−vis analyses could be directly performed. Electrochemical characterizations were carried out under conditions similar to those of electrogeneration. In some of these tests the potential was scanned up to higher values, to estimate the overoxidation potential, and at quite negative values, with the aim of checking the possible occurrence of a n-doping process.

Figure 6 shows typical *i*/*E* curves recorded during electrogeneration−deposition on the Pt electrode of **P1E**. Qualitatively similar curves are recorded for **P2E**. Two anodic−cathodic peak systems are detectable, the less anodic one being much sharper and the latter one being very broad. As Figure 6 shows, voltammograms subsequently recorded during potential scans between 0.00 and +1.00 V exhibit typically increasing height of both the anodic and the directly associated cathodic peaks, which is explained admitting that p-doping, which makes the polymer coverage conductive, takes place at less anodic potentials than those at which the polymer deposit forms.[25] Actually, monomer oxidation and polymer growth only occur at potentials as high as +1.00 and +1.10 V for **P1E** and **P2E**, respectively.

Consistent results are collected from the electrochemical characterization of the deposit, performed by dipping the modified electrode into a MeCN solution only containing the supporting electrolyte (Figure 7 for **P1E**). The cathodic peaks are both attributable to the discharge of the polymer that becomes nonconductive at potentials lower than about +0.40 and +0.70 V vs SCE for **P1E** and **P2E**, respectively. Since the peak potential values of both the anodic and the cathodic peaks depend on the thickness of the coatings, due to the progressively increasing resistance introduced into the film by the counterion migration, the values in Table 3 only assume indicative and comparative meaning. They are measured after 50 potential cycles between 0.00 and +1.00 or +1.10 V, at a scan rate of 50 mV s^{-1}, on 5×10^{-3} M monomer solutions. It is noteworthy that for both **P1** and **P2** the useful potential range in which the polymer is reversibly p-doped is quite wide, since overoxidation, leading to irreversible modification, only takes place at potentials more anodic than 1.50 V. This is a particularly appealing peculiarity of the studied polymers.

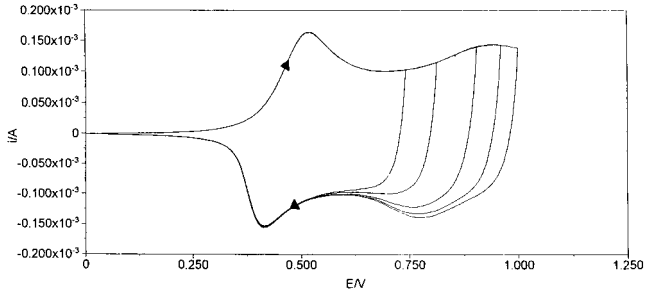

Figure 7. Cyclic voltammogram of film of electrogenerated polymer **P1E.** Ag|AgCl(s),KCl(s) reference electrode; 50 mV s^{-1} potential scan rate; initial anodic scan direction.

Table 3. Peak Potential Values for Charge−Discharge Processes[a]

	P1E	P2E
$E_{p,a,1}$	+0.51 (+0.63)	+0.80 (+0.82)
$E_{p,c,1}$	+0.41 (+0.55)	+0.74 (+0.74, +0.63)
$E_{p,a,2}$	+0.95 (+0.83)	+0.97 (−)
$E_{p,c,2}$	+0.78 (+0.74)	+0.92 (−)

[a] Values in volts; SCE reference electrode. Potential values for chemically prepared coatings in parentheses.

The current/potential curves relative to **P2E** coverages are affected by quite a remarkable noise superimposed on a well-reproducible signal. It is difficult to give at the moment a rationale for this noise, which is absent when examining the same polymer synthesized by conventional chemical methods. Considering that an analysis of the spectrum of the signal does not show any gap between the useful frequencies and those attributable to "noise", which is, on the contrary, the situation typical of instrumental high-frequency noise, it could be explained by a poor adherence of the film formed on the electrode: however, alternative hypotheses could be an intrinsic difference in the crystal status of the two polymers or the inclusion of solvent droplets either into the growing polymer or between the electrode and the polymer surfaces "in contact" with each other. Studies with suitable surface techniques will hopefully allow us to clarify this unusual behavior.

Electrochemical characterization of the polymer prepared by chemical methods was performed by dissolving a weighted amount of solid polymer in a known volume of $CHCl_3$ and then dropping 30 μL of the resulting solution on the electrode surface. The modified electrode was then carefully dried at 35 °C under reduced pressure. For **P1** a voltammetric pattern similar to that of the electrogenerated polymer is obtained, even if the differences in the peak potential values are significant

(see Table 3). For **P2** obtained by the chemical method only the first oxidation is recorded, two related discharge responses being evidenced. However, considering the broadness of the more anodic response recorded on the electrochemically generated coverages, this is not a difference to overestimate. Furthermore, when electrogenerating the polymers on ITO glass, the UV−vis spectra recorded resulted similar to those of the corresponding polymer prepared by chemical oxidation and deposited on the glass, giving an indication of the similarity between the products of the two processes.

Particularly interesting are the results of preliminary tests performed polarizing the coated electrodes at negative potential values. A cathodic response attributable to n-doping is observed in the case of **P1**. In particular, the polymer prepared by electroxidation is more easily reducible, so that the relevant charge−discharge process (i.e., the cathodic−anodic peak system) is better resolved with respect to the solvent discharge. This aspect deserves more careful studies, also using different supporting electrolytes.

Discussion

Some remarks about the oxidative polymerization of symmetrical bis(alkylsulfanyl)bithiophenes are to be made. The oxidative coupling with $FeCl_3$ of TT β,β'-bis(alkylsulfanyl)bithiophenes produces polybithiophenes, **P1** and **P2**, of much higher M_w than that reported for poly[3,3′-bis(butylsulfanyl)-2,2′-bithiophene]s by nickel-catalyzed Grignard cross-coupling[8a] and by oxidative polymerization with $FeCl_3$.[9] UV−vis spectra of **P1** and **P2** show a λ_{max} at a longer wavelength with respect to the former polymer, but at the same value of the latter. In principle, the 3,3′-bis(butylsulfanyl)- and 4,4′-bis(butylsulfanyl)-2,2′-bithiophene should generate the same polymers, and the differences observed can be due to the different polymerization method or to the different reactivity of the starting bithiophenes.

To clarify the different behavior of HH and TT β,β'-bis(alkylsulfanyl)bithiophenes, we investigated the nickel-catalyzed Grignard cross-coupling reaction of 4,4′-bis(butilsulfanyl)-2,2′-bithiophene and the oxidative coupling of 3,3′-bis(butylsulfanyl)-2,2′-bithiophene by means of $FeCl_3$. The cross-coupling reaction of the di-Grignard reagent of 5,5′-diiodo-4,4′-bis(butylsulfanyl)-2,2′-bithiophene afforded a polymer with M_w of 6 kDa, a value comparable to that obtained by oxidative method, but the ^1H NMR spectrum displays, in the aromatic region, in addition to a sharp peak at 7.20 ppm, attributable to H-3 of the thiophene ring, other signals due to unseparable oligomeric fractions. Moreover, the very low peak corresponding to aromatic C−H_β stretching in the IR spectrum indicates the presence of some percentage of $\alpha-\beta$ linkages, and the NMR spectra display groups of not well-resolved signals, indicative of the presence of oligomeric chains. Furthermore, this polymer does not present solvatochromic properties, denoting the presence of species with low regioregularity.

These results, together with those reported in ref 8a for 3,3′-bis(butylsulfanyl)-2,2′-bithiophene, suggest that the chemical polymerization, via nickel-catalyzed Grignard cross-coupling, starting from either 4,4′-bis(butylsulfanyl)- or 3,3′-bis(butylsulfanyl)-2,2′-bithiophene, produces polymers with spectroscopic characteristics less satisfactory than those presented by **P1** and **P2**. The pendant groups seem to affect markedly the reactivity of the dihalo derivative during the formation of the di-Grignard reagent.

Preliminary tests carried out in our laboratory on the oxidative polymerization with $FeCl_3$ of 3,3′-bis(butylsulfanyl)-2,2′-bithiophene in $CHCl_3$ afforded, as the main product, a hexasubstituted sexithiophene,[26] whereas the same reaction has been recently reported to give a low-M_w poly[3,3′-bis(butylsulfanyl)-2,2′-bithiophene],[9] with the same optical properties of **P1** and **P2**.

The different behavior of the 3,3′-bis(butylsulfanyl)-2,2′-bithiophene with respect to the 4,4′-bis(butylsulfanyl)-2,2′-bithiophene in the oxidative polymerization can be explained by considering the different conjugational ability of the butylsulfanyl group which reflects on the stability of the radical cation formed during the polymerization process. In fact, the lone pairs of the sulfur atoms in 3- and 3′-positions can be delocalized over the whole molecular skeleton, stabilizing the radical cation, whereas the outer butylsulfanyl groups, placed in 4- and 4′-positions, can only give rise to a less extended conjugation pattern, giving more reactive species.[13,27]

Conclusion

Two regioregular HH−TT polybithiophenes β,β'-difunctionalized with alkylsulfanyl chains of different length (butyl- and octylsulfanyl) were studied. The octylsulfanyl group favors the synthesis of a free-standing polymer **P2**, with an average-weight molecular weight of 70 kDa, which possesses flexibility and strength, and can be easily manipulated and cut. Moreover, it retains a good solubility in common organic solvents, such as $CHCl_3$, CH_2Cl_2, CCl_4, CS_2, benzene, toluene, and THF. The polymer **P1**, bearing butylsulfanyl groups in the β-position, presents spectroscopic characteristics very similar to those of **P2**, though having lower M_w and consistency. Poly[4,4′-bis(alkylsulfanyl)-2,2′-bithiophene]s present a higher polymerization degree than HT poly[3-(alkylsulfanyl)thiophene]s[2] and poly[3,3′-bis(butylsulfanyl)-2,2′-bithiophene]s.[8a,9]

As for the electrochemical polymerization of **2a** and **2b**, we have checked that polymers similar to those prepared chemically are formed. The possibility of better controlling the experimental conditions (monomer concentration, nature of supporting electrolyte, potentiodynamic or potentiostatic oxidation, doping potential, and others) deserves to be capitalized in order to fully explore the variability of the characteristics of **P1E** and **P2E**.

Acknowledgment. The authors are grateful to the Italian MURST for financial support. Thanks are due to the Centro Interdipartimentale Grandi Strumenti of University of Modena for the use of the Bruker AMX-400 WB and Bruker Avance DPX-200 spectrometers, Perkin-Elmer TGA7 instrument, the Perkin-Elmer i-series FT-IR, and the Park Autoprobe CP scanning probe microscopes.

References and Notes

(1) McCullough, R. D. *Adv. Mater.* **1998**, *10*, 93−116.
(2) Wu, X.; Chen, T.-A.; Rieke, R. D. *Macromolecules* **1996**, *29*, 7671−7677.
(3) (a) Zargoska, M.; Kulszewics-Bajer, I.; Pron, A.; Firlej, L.; Bernier, P.; Galtier, M. *Synth. Met.* **1991**, *45*, 385−393. (b) Louarn, G.; Kruszka, J.; Lefrant, S.; Zargoska, M.; Kulszewics-Bajer, I.; Pron, A. *Synth. Met.* **1993**, *61*, 233−238.
(4) Souto Maior, R. M.; Hinkelmann, K.; Eckert, H.; Wudl, F. *Macromolecules* **1990**, *23*, 1268−1279.
(5) Faïd, K.; Cloutier, R.; Leclerc, M. *Macromolecules* **1993**, *26*, 2501−2507.

(6) Wu, X.; Chen, T.-A.; Rieke, R. D. *Macromolecules* **1995**, *28*, 2101−2102.
(7) Goldoni, F.; Iarossi, D.; Mucci, A.; Schenetti, L.; Zambianchi, M. *J. Mater. Chem*. **1997**, *7*, 593−596.
(8) (a) Ng, S. C.; Chan, H. S. O.; Miao, P.; Tan, K. L. *Synth. Met*. **1997**, *90*, 25−30. (b) Ng, S. C.; Miao, P.; Chan, H. S. O. *Chem. Commun*. **1998**, 153−154.
(9) Raymond, F.; Di Césare, N.; Belletête, M.; Durocher, G.; Leclerc, M. *Adv. Mater*. **1998**, *10*, 599−602.
(10) Folli, U.; Goldoni, F.; Iarossi, D.; Mucci, A.; Schenetti**,** L. *J. Chem. Res*. **1996**, 69.
(11) Ng, S. C.; Chan, H. S. O.; Huang, H. H.; Swee-How, R. *J. Chem. Res*. **1996**, 232.
(12) Goldoni, F.; Iarossi, D.; Mucci, A.; Schenetti, L. *Chem. Commun*. **1997**, 2175−2176.
(13) Barbarella, G.; Zambianchi, M.; Di Toro, R.; Colonna, M., Jr.; Iarossi, D.; Goldoni, F.; Bongini, A. *J. Org. Chem*. **1996**, *61*, 8285−8292.
(14) Bax, A.; Griffey, R. H.; Hawkins, B. L. *J. Magn. Reson*. **1983**, *55*, 301−315.
(15) Bax, A.; Summers, M. F. *J. Am. Chem. Soc*. **1986**, *108*, 2093−2094.
(16) Antolini, L.; Goldoni, F.; Iarossi, D.; Mucci, A.; Schenetti, L. *J. Chem. Soc., Perkin Trans. 1* **1997**, 1957−1961.
(17) Goldoni, F.; Iarossi, D.; Mucci, A.; Schenetti, L.; Costa Bizzarri, P.; Della Casa, C.; Lanzi, M. *Polymer* **1997**, *38*, 1297−1302 and references therein.
(18) (a) Rughooputh, S. D. D. V.; Hotta, S.; Heeger, A. J.; Wudl, F. *J. Polym. Sci., Polym. Phys. Ed*. **1987**, *25*, 1071−1078. (b) Salaneck, W. R.; Inganäs, O.; Thémans, B.; Nilsson, J. O.; Sjögren, B.; Österholm, J.-E.; Brèdas, J.-L.; Svensson, S. *J. Chem. Phys*. **1988**, *89*, 4613−4619. (c) Tashiro, K.; Minagawa, Y.; Kobayashi, M.; Morita, S.; Kawai, T.; Yoshino, K. *Synth. Met*. **1993**, *55*, 321−328. (d) Faïd, K.; Fréchette, M.; Ranger, M.; Mazerolle, L.; Lévesque, I.; Leclerc, M.; Chen, T.-A.; Rieke, R. D. *Chem. Mater*. **1995**, *7*, 1390−1396. (e) Leclerc, M.; Fréchette, M.; Bergeron, J. Y.; Ranger, M.; Lévesque, I.; Faïd, K. *Macromol. Chem. Phys*. **1996**, *197*, 2077−2087. (f) Bouman, M. M.; Meijer, E. W. *Adv. Mater*. **1995**, *7*, 385−387. (g) Langeveld-Voss, B. M. W.; Bouman, M. M.; Christiaans, M. P. T.; Janssen, R. A. J.; Meijer, E. W. *Polym. Mater. Sci. Eng*. **1996**, *37*, 499−500. (h) Leclerc, M.; Faïd, K. *Adv. Mater*. **1997**, *9*, 1087−1094.
(19) (a) Roux, C.; Bergeron, J. Y.; Leclerc, M. *Makromol. Chem*. **1993**, *194*, 869−877. (b) Bouman, M. M.; Havinga, E. E.; Janssen, R. A. J.; Meijer, E. W. *Mol. Cryst. Liq. Cryst*. **1994**, *256*, 439−448.
(20) Chen, A.; Wu, X.; Rieke, R. D. *J. Am. Chem. Soc*. **1995**, *117*, 233−244.
(21) (a) McCullough, R. D.; Williams, S. P. *J. Am. Chem. Soc*. **1993**, *115*, 11608-11609. (b) McCullough, R. D.; Williams, S. P.; Tristram-Nagle, S.; Jayaraman, M.; Ewbank, P. C.; Miller, L. *Synth. Met*. **1995**, *69*, 279−282.
(22) Di Césare, N.; Belletête, M.; Durocher, G.; Leclerc, M. *Chem. Phys. Lett*. **1997**, *275*, 533−539.
(23) Green, M. A.; Gunn, N. W. *Solid State Electron*. **1971**, *14*, 1167−1177.
(24) Zargóska, M.; Krische, B. *Polymer* **1990**, *21*, 1379−1383.
(25) Heinze, J. in *Topics in Current Chemistry*; Springer: Berlin, 1990; Vol. 152, pp 1−47.
(26) Work in progress.
(27) Smie, A.; Synowczyk, A.; Heinze, J.; Alle, R.; Tschuncky, P.; Götz, G.; Bäuerle, P. *J. Electroanal. Chem*. **1998**, *452*, 87−95.

MA9813340